

# Simple model of Feshbach resonance in the strong-coupling regime

T. Wasak, M. Krych, Z. Idziaszek and M. Trippenbach

*Faculty of Physics, University of Warsaw, ul. Hoża 69, PL-00-681 Warszawa, Poland*

Y. Avishai

*Department of Physics and the Ilse Katz Center for Nano-Science,  
Ben-Gurion University, Beer-Sheva 84105, Israel*

Y. B. Band

*Department of Chemistry, Department of Physics and Department of Electro-Optics,  
and the Ilse Katz Center for Nano-Science, Ben-Gurion University, Beer-Sheva 84105, Israel*

We use the dressed potentials obtained in the adiabatic representation of two coupled channels to calculate  $s$ -wave Feshbach resonances in a 3D spherically symmetric potential with an open channel interacting with a closed channel. Analytic expressions for the  $s$ -wave scattering length  $a$  and number of resonances are obtained for a piecewise constant model with a piecewise constant interaction of the open and closed channels near the origin. We show analytically and numerically that, for strong enough coupling strength, Feshbach resonances can exist even when the closed channel does *not* have a bound state.

PACS numbers:

## I. INTRODUCTION

Resonance scattering phenomena are ubiquitous; they have been observed in many different physical scenarios, including electronic transport and optical spectra in semiconductors [1–3], collisions of ultracold atoms [4] and creation of ultracold molecules [5]. Herman Feshbach [6] and Ugo Fano [7] developed theoretical methods to treat resonance phenomena that arise from the coupling of a discrete state to the continuum. This type of resonance scattering was first modeled in the context of the autoionization of atoms [7]. The term Feshbach resonance (FR), sometimes also called Fano-Feshbach resonance, is now most often used to describe scattering processes wherein a bound state on a “closed channel” strongly affects the scattering on an open scattering channel which is weakly coupled to the bound state; flux entering the open channel gets temporarily caught in the closed channel bound state, before eventually leaking back to the open channel. The use of FR scattering to affect the low energy collisions of atoms has become an important experimental tool for controlling the properties of low temperature atomic and molecular gases [4]. Thus, the magnitude and sign of the low-energy atomic interactions can be varied by coupling free particles to a molecular state [8, 9], thereby tuning the properties of the many-body gas. Mostly, magnetic field induced Feshbach scattering resonances have been employed experimentally. In addition, FRs can also be controlled optically [10, 11] or with the help of electric fields [12]. For example, scattering resonances arise under the influence of laser light tuned near a photoassociation resonance, where free atom pairs are coupled to an excited molecular state [13].

In this work we introduce a FR model for 3D scattering from centrally symmetric piecewise constant open and closed channel potentials with a constant interaction

over the inner part of the potentials. The model admits an analytic solution that allows for a full understanding of the various aspects of FR scattering that have heretofore not been explored. Specifically, we show that a new regime of FRs exists wherein a closed channel with a *repulsive potential* [23] can give rise to FRs when the interaction coupling strength is sufficiently strong; in this regime, FRs can exist even when the closed channel does not have a bound state. The present analysis complements the tight-binding model and the formal scattering theory results published in Ref. [14], square well model presented in Ref. [21] and atomic waveguide model from Ref. [22], and demonstrates that a FR with a closed channel that does not have a bound state is not an artifact of the tight-binding model.

The outline of this manuscript is as follows. In Sec. II the basic equations defining the FR physics are presented. In Sec. III we specify the model, define the piecewise-constant coupling model and introduce the dimensionless units used in the manuscript. Section IV solves the coupled channel Schrödinger equation for bound states. The analytic formula for the scattering length is derived in Sec. V. Section VI presents the adiabatic representation and the bound states that appear in the “dressed” potentials of this representation (the dressing is due to the interaction between channels). In Sec. VII we present a detailed analysis of the resonances in the strong coupling regime. Finally, a summary and conclusion are provided in Sec. VIII.

## II. BASIC EQUATIONS DEFINING FESHBACH RESONANCE PHYSICS

We consider two coupled channels, the open channel  $o$  and the closed channel  $c$ . The wave functions  $\psi_o$  and  $\psi_c$

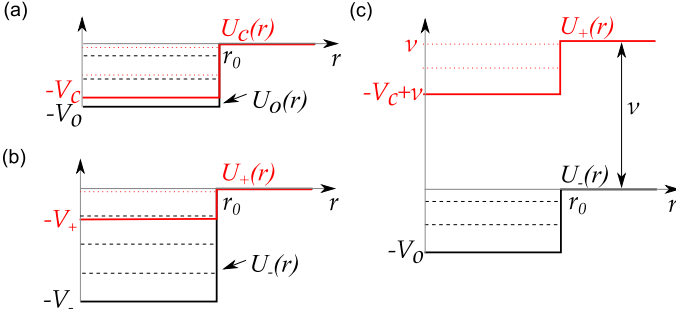


FIG. 1: (Color online) Dressed potential picture of coupled channel model for piecewise constant potential. (a) The level structure of original potentials  $U(r)$ . Open channel  $U_o(r)$  and closed channel  $U_c(r)$  (coupling  $\tau = 0$  and detuning  $\nu = 0$ ). (b) Dressed potentials  $U_+(r)$  and  $U_-(r)$  for non-vanishing coupling,  $\tau > 0$ , and asymptotic potential energy difference  $\nu = 0$ . (c) Same as (b) but for  $\nu \gg 0$ . In all panels, dashed lines denote bound states of the  $U_o(r)$  and  $U_-(r)$  potentials and dotted lines correspond to  $U_c(r)$  and  $U_+(r)$ . All length variables are expressed in units of  $r_0$  and all energies are given in units of  $\hbar^2/(2mr_0^2)$ .

satisfy Schrödinger equation,

$$\left(-\frac{\hbar^2}{2m}\nabla^2 + U_o(\mathbf{r})\right)\psi_o(\mathbf{r}) + U_{oc}(\mathbf{r})\psi_c(\mathbf{r}) = E\psi_o(\mathbf{r}) \quad (1)$$

$$\left(-\frac{\hbar^2}{2m}\nabla^2 + U_c(\mathbf{r})\right)\psi_c(\mathbf{r}) + U_{co}(\mathbf{r})\psi_o(\mathbf{r}) = E\psi_c(\mathbf{r}) \quad (2)$$

We assume that the open channel potential  $U_o(\mathbf{r})$  vanishes as  $|\mathbf{r}| \rightarrow \infty$ , i.e., the open channel asymptote defines the zero of potential energy. The closed channel potential  $U_c(\mathbf{r})$  tends asymptotically to a positive constant  $\nu > 0$ . We further assume that the coupling potential  $V_{oc}(\mathbf{r})$  is real. Figure 1(a) shows a schematic illustration of the open and closed potentials,  $U_o$  and  $U_c$ , which will be fully specified in Sec. III.

### III. PIECEWISE-CONSTANT COUPLING

We use a square well model with piecewise constant potentials of the form (see Fig. 1),

$$U_o(r) = \begin{cases} 0 & \text{if } r > r_0 \\ -V_o & \text{if } r < r_0 \end{cases}, \quad (3)$$

$$U_c(r) = \begin{cases} \nu & \text{if } r > r_0 \\ -V_c + \nu & \text{if } r < r_0 \end{cases}, \quad (4)$$

with  $\nu \geq 0$ , and that the open and closed channels are coupled inside the well (see, e.g., Ref. [20]),

$$U_{oc}(r) = g\theta(1 - |r_0|), \quad (5)$$

where  $\theta$  is the step function and the coupling interaction strength  $g$  is real. The Schrödinger equation for the  $s$ -wave radial functions  $u_{o,c}(r) = r\psi_{o,c}(r)$  with energy  $E$

is

$$-\frac{\hbar^2}{2m}u_o''(\rho) + (U_o(\rho) - E)u_o(\rho) + U_{oc}(\rho)u_c(\rho) = 0, \quad (6)$$

$$-\frac{\hbar^2}{2m}u_c''(\rho) + (U_c(\rho) - E)u_c(\rho) + U_{oc}(\rho)u_o(\rho) = 0. \quad (7)$$

The energy scales in the model can be related to the wavenumbers. Below we use the dimensionless wavenumbers related to the energies by the energy-momentum relations:  $\kappa = \sqrt{2mr_0^2 E}/\hbar$ ,  $\kappa_{o,c} = \sqrt{2mr_0^2 V_{o,c}}/\hbar$ , and  $\kappa_\nu = \sqrt{2mr_0^2 \nu}/\hbar$ , where  $\nu$  is the asymptotic potential energy difference and  $m$  is a reduced mass. Moreover, all length variables will hereafter be expressed in units of  $r_0$  and all energies will be given in units of  $\hbar^2/(2mr_0^2)$ . We also use a dimensionless coupling strength  $\tau = (2mr_0^2 g)/\hbar^2$ , dimensionless scattering lengths,  $\alpha = a/r_0$  and  $\alpha_{bg} = a_{bg}/r_0$ , and a dimensionless radial coordinate  $\rho = r/r_0$ .

### IV. COUPLED CHANNEL SCHRÖDINGER EQUATION: BOUND STATES

The Schrödinger equation for the square well model introduced in Sec. III can be solved analytically [20]. For  $\rho > 1$ , the inter-channel coupling is zero, and the Schrödinger equations for bound states can be written as

$$-\partial_\rho^2 u_o = -\kappa^2 u_o, \quad (8)$$

$$(-\partial_\rho^2 + \kappa_\nu^2)u_c = -\kappa^2 u_c, \quad (9)$$

and their solutions are,

$$u_o(\rho) = A_o e^{-\kappa\rho},$$

$$u_c(\rho) = A_c e^{-\sqrt{\kappa^2 + \kappa_\nu^2}\rho}. \quad (10)$$

In the region where the channels are coupled,  $\rho < 1$ , the equations are,

$$(-\partial_\rho^2 - \kappa_o^2)u_o + \tau u_c = -\kappa^2 u_o,$$

$$(-\partial_\rho^2 - \kappa_c^2 + \kappa_\nu^2)u_c + \tau u_o = -\kappa^2 u_c. \quad (11)$$

To solve Eqs. (11) we introduce the superposition states

$$v_o = c u_o - s u_c, \quad v_c = s u_o + c u_c,$$

where  $c \equiv \cos\theta$ ,  $s \equiv \sin\theta$ , and

$$\tan(2\theta) = -\frac{2\tau}{(\kappa_o^2 - \kappa_c^2 + \kappa_\nu^2)}, \quad (12)$$

and we obtain the set of uncoupled equations,

$$(\partial_\rho^2 + c^2 \kappa_o^2 + s^2 (\kappa_c^2 - \kappa_\nu^2) - \kappa^2 - 2\tau s c) v_o = 0, \quad (13)$$

$$(\partial_\rho^2 + s^2 \kappa_o^2 + c^2 (\kappa_c^2 - \kappa_\nu^2) - \kappa^2 + 2\tau s c) v_c = 0. \quad (14)$$

Note that the mixing angle  $\theta$  does not depend on energy; it only depends on the potentials and coupling strength  $\tau$ . We define two auxiliary quantities,

$$\begin{aligned}\xi_1 &= \sqrt{c^2(\kappa_o^2 - \kappa^2) + s^2(\kappa_c^2 - \kappa^2 - \kappa_\nu^2) - 2\tau sc}, \\ \xi_2 &= \sqrt{s^2(\kappa_o^2 - \kappa^2) + c^2(\kappa_c^2 - \kappa^2 - \kappa_\nu^2) + 2\tau sc}\end{aligned}$$

and notice that they can be either real or pure imaginary. Using the above definitions, the solution of the differential equations (13) and (14) are,

$$v_o(\rho) = C_o \sin(\xi_1 \rho), \quad v_c(\rho) = C_c \sin(\xi_2 \rho), \quad (15)$$

which satisfy boundary conditions,  $v_o(0) = v_c(0) = 0$ . In order to obtain the energy of the bound states and the scattering length of the coupled system, we consider the following form of the wave functions  $u_o(\rho)$  and  $u_c(\rho)$ :

$$\begin{aligned}u_o(\rho) &= cC_o \sin(\xi_1 \rho) + sC_c \sin(\xi_2 \rho), \quad \text{for } \rho < 1 \\ u_o(\rho) &= A_o e^{-\kappa \rho}, \quad \text{for } \rho > 1 \\ u_c(\rho) &= -sC_o \sin(\xi_1 \rho) + cC_c \sin(\xi_2 \rho), \quad \text{for } \rho < 1 \\ u_c(\rho) &= A_c e^{-\sqrt{\kappa^2 + \kappa_\nu^2} \rho}, \quad \text{for } \rho > 1.\end{aligned} \quad (16)$$

Note that in order to determine the scattering length, one has to take wavefunction for the zero energy, and for  $\rho > 1$ ,  $u_o(r) = A_o(\rho - \alpha)$ .

To determine the bound states, we match the logarithmic derivatives of  $u_o$  and  $u_c$  at  $\rho = 1$ , assuming  $\kappa > 0$ , and thereby obtain the two conditions,

$$\begin{aligned}\frac{cC_o \xi_1 \cos(\xi_1) + sC_c \xi_2 \cos(\xi_2)}{cC_o \sin(\xi_1) + sC_c \sin(\xi_2)} &= -\kappa, \quad (17) \\ \frac{-sC_o \xi_1 \cos(\xi_1) + cC_c \xi_2 \cos(\xi_2)}{-sC_o \sin(\xi_1) + cC_c \sin(\xi_2)} &= -\sqrt{\kappa^2 + \kappa_\nu^2}.\end{aligned} \quad (18)$$

We can extract  $C_c/C_o = s\zeta_b/c$  from the first of these equations. Defining  $\zeta_b$ , we find,

$$\zeta_b = -\frac{\xi_1 \cos(\xi_1) + \kappa \sin(\xi_1)}{\xi_2 \cos(\xi_2) + \kappa \sin(\xi_2)}, \quad (19)$$

and then inserting this ratio into the second equation to obtain an expression for energy  $E = -\hbar^2 \kappa^2 / (2mr_0^2)$ , we obtain

$$\sqrt{\kappa^2 + \kappa_\nu^2} = \frac{s^2 \xi_1 \cos(\xi_1) + c^2 \zeta_b \xi_2 \cos(\xi_2)}{s^2 \sin(\xi_1) + c^2 \zeta_b \sin(\xi_2)}. \quad (20)$$

To obtain the values of the energies of the eigenstates of the coupled system, Eq. (20) needs to be solved for  $\kappa$ .

## V. THE SCATTERING LENGTH

To determine the scattering length, we match the logarithmic derivatives of the zero energy ( $\kappa = 0$ ) wavefunctions  $u_o$  and  $u_c$  at  $\rho = 1$ , and find,

$$\left. \frac{u'_o(1^-)}{u_o(1^-)} \right|_{\kappa=0} = \frac{1}{1 - \alpha}, \quad (21)$$

$$\left. \frac{u'_c(1^-)}{u_c(1^-)} \right|_{\kappa=0} = -\kappa_\nu. \quad (22)$$

From Eq. (22), we obtain  $\zeta_a$ , defined by relation  $C_c/C_o = s\zeta_a/c$ :

$$\zeta_a = \frac{\xi_1 \cos(\xi_1) + \sqrt{\kappa^2 + \kappa_\nu^2} \sin(\xi_1)}{\xi_2 \cos(\xi_2) + \sqrt{\kappa^2 + \kappa_\nu^2} \sin(\xi_2)}. \quad (23)$$

Using Eq. (21), an expression for the scattering length, expressed in terms of  $\zeta_a$ , is obtained:

$$\alpha = 1 - \frac{c^2 \sin(\xi_1) + s^2 \zeta_a \sin(\xi_2)}{c^2 \xi_1 \cos(\xi_1) + s^2 \zeta_a \xi_2 \cos(\xi_2)} \Big|_{\kappa=0}. \quad (24)$$

## VI. ADIABATIC REPRESENTATION

We determine the number of FRs for the whole range of asymptotic potential energy differences between the coupled channels,  $\nu$ . We use the adiabatic representation in which the Hamiltonian describing the problem [Eqs. (8) and (11)] is transformed unitarily to make the potential matrix diagonal. For piecewise constant interaction potentials, the kinetic energy operator remains diagonal. The eigenvalues of the potential energy matrix, denoted by  $U_\pm$ , are such that

$$0 = \det \begin{pmatrix} U_o - U_\pm & U_{oc} \\ U_{oc} & U_c - U_\pm \end{pmatrix} \quad (25)$$

The eigenvalues for  $r < r_0$  are  $-V_\pm$ , where

$$V_\pm = \frac{V_o + V_c - \nu}{2} \mp \sqrt{\left( \frac{-V_o + V_c - \nu}{2} \right)^2 + V_{oc}^2}. \quad (26)$$

In case of the piecewise constant potential with piecewise constant coupling, the adiabatic representation yields an exact solution everywhere. Notice that adiabatic transformation matrix is constant and commutes with the kinetic energy operator. Equation (26) describes two effective potentials. The stronger the coupling between the channels, the larger is the change in the well depth. The higher energy potential is shifted upwards by the same amount as the lower one is shifted downwards. This can result in the emergence of new bound states in the lower channel and their vanishing in the upper one (cf., Fig. 1).

It is important to analyze the depth of the potentials  $V_+$  and  $V_-$  in order to establish their bound state structure. From Eq. (26) we conclude that they depend both on the coupling  $V_{oc}$  and the detuning  $\nu$ . In Fig. 2 we plot both  $V_+$  and  $V_-$  as a function of the detuning for two cases, depending on which of the potentials, open or closed, is deeper, assuming they are both attractive. In Fig. 2(a) the potential well in the open channel is deeper, and when we turn on interactions, the dressed potential  $V_-$  is shifted downwards from  $V_o$  and  $V_+$  is shifted upwards from  $V_c$ . Imagine that we fix  $V_{oc}$  (later we use  $\tau$  instead) and increase  $\nu$ . The potential  $V_-$  will converge back to  $V_o$  as  $\nu$  is increased, and any bound states that

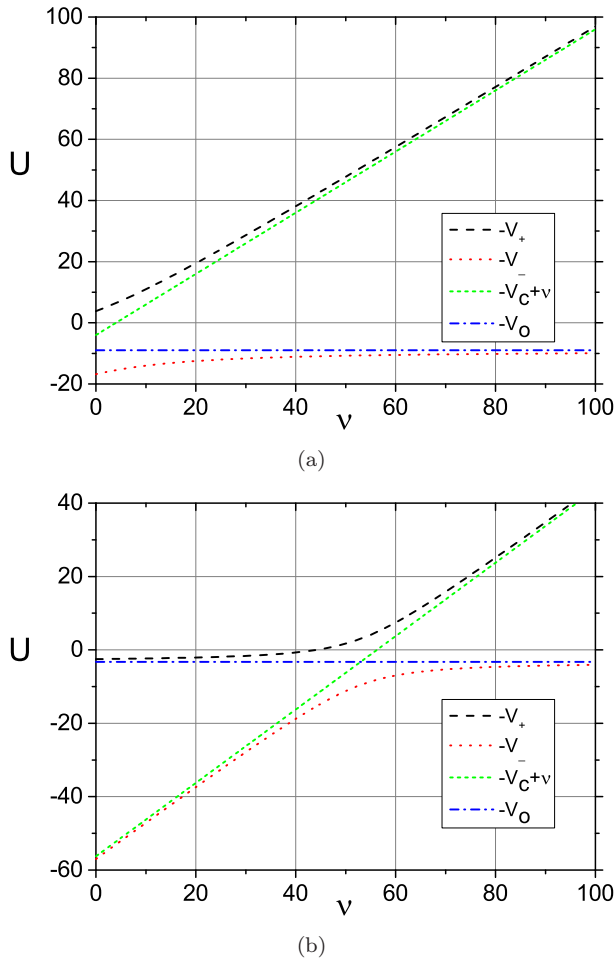


FIG. 2: (Color online) The depth of the dressed potentials versus the detuning  $\nu$ , depending on the relative depth of  $V_o$  and  $V_c$ . (a)  $V_c < V_o$ , and in particular  $\kappa_o = 3$ ,  $\kappa_c = 2$ ,  $\tau = 10$  (b)  $V_o < V_c$  ( $\kappa_o = 1.8$ ,  $\kappa_c = 7.5$ ,  $\tau = 6.3$ ), where the avoided crossing is clearly seen. All energies are given in units of  $\hbar^2/(2mr_0^2)$ .

may have been created at  $\nu = 0$  due to the interaction that deepens the well will eventually be pushed out when the detuning  $\nu$  becomes large. Consequently  $V_+$  will eventually approach  $V_c + \nu$ , and if the interaction pushes out bound states at  $\nu = 0$  from the  $V_c$  potential into continuum, they will eventually come back at large  $\nu$ . These observations are crucial for further analysis, as we claim below that bound states appear whenever a FR from the continuum is pushed under the dissociation threshold, and similarly, FRs appear whenever a bound state from the continuum is pushed out of the channel.

The situation is somewhat more complicated when the closed channel potential is deeper than the open channel potential, as illustrated in Fig 2(b). Now  $V_-$  starts below  $V_c$  for small detuning and  $V_+$  is above  $V_o$  when the coupling is first turned on. As we increase the detuning  $\nu$ , holding the coupling strength fixed, we observe an avoided crossing:  $V_-$  tends to  $V_o$  and  $V_+$  tends to

$V_c + \nu$ . This case is carefully analyzed in conjunction with our numerical studies reported in the next section. The above considerations allow us to determine the depth of the dressed potentials and hence to find the number of bound states in each of them for different values of the strength and the detuning parameter  $\nu$ .

The number of  $s$ -wave bound states in the three-dimensional potential well of depth  $V$ ,  $n$ , is known to be equal to the value of the floor function for  $n^*$ , i.e., the largest natural number smaller or equal to  $n^*$ , which is defined by the formula:

$$V = \frac{\hbar^2}{2mr_0^2} \left(\frac{\pi}{2}\right)^2 (2n^* - 1)^2. \quad (27)$$

Note that  $n^*$  is in general not an integer. In the above formula we deliberately did not use dimensionless parameters. Consider the case where the weakest bound state is just below threshold, i.e., the potential  $V$  is tuned such that there is a pole of the Green's function at  $E = E_b \approx 0^-$ , where  $E_b$  is the binding energy of the bound state. As  $V$  is slowly decreased, at some value of the potential,  $V_{\text{th}}$ , the pole of the Green's function crosses threshold an energy  $E_r \approx 0^+$ . For a scattering energy  $E = E_r$  there is a zero energy resonance. Before crossing threshold, i.e., for  $V > V_{\text{th}}$ , the approximate formula for the scattering length is  $a \approx \hbar/\sqrt{2m|E_b|}$ ; this formula is valid close to threshold [24]. Exactly at the point when one of the bound states crosses threshold,  $n^*$  becomes an integer and the number of bound states, including the one leaving the potential well, is precisely equal to  $n = n^*$ . Consequently, by equating the potential depth in Eq. (27) to  $V_{\pm}$  in Eq. (26) and setting  $\nu = 0$ , we can derive a formula for the threshold value of the coupling strength  $\tau_{\text{th}}$ , which constitutes the boundary between regions in  $\kappa_c$ - $\kappa_o$  space where the number of bound states increases or decreases by one. In dimensionless units  $\tau_{\text{th}}$  is given by

$$\tau_{\text{th}}^2 = \left[ \left(\frac{\pi}{2}\right)^2 (2n - 1)^2 - \kappa_o^2 \right] \left[ \left(\frac{\pi}{2}\right)^2 (2n - 1)^2 - \kappa_c^2 \right]. \quad (28)$$

As seen from the above equation, there are two possibilities:  $\left(\frac{\pi}{2}\right)^2 (2n - 1)^2 \geq \kappa_o^2$  and  $\left(\frac{\pi}{2}\right)^2 (2n - 1)^2 \geq \kappa_c^2$  or  $\left(\frac{\pi}{2}\right)^2 (2n - 1)^2 < \kappa_o^2$  and  $\left(\frac{\pi}{2}\right)^2 (2n - 1)^2 < \kappa_c^2$ . The first (second) describes the solid (dashed) lines on Fig. 6 and depicts the emergence (vanishing) of the bound states in the lower (higher) channel with the increasing coupling. In the case of a repulsive potential in the closed channel, there are no bound states, but Eq. (28) is still valid (cf., Fig. 3).

Let us analyze the number of bound states in the dressed effective potentials from the point of view of FRs. The coupling of the channels with strength  $\tau$  and the shifting of the one channel potential relative to the other by changing the asymptotic potential energy difference  $\nu$  can be considered as a two-step process depicted in Fig. 1 (a)-(c). In the first step, increase  $\tau$  but keep  $\nu = 0$ .

The deeper of the potential wells becomes even deeper and a new bound state will eventually appear in the adiabatic picture as  $\tau$  is increased. On the other hand, the upper channel potential well becomes shallower and its bound states (if present) can be pushed away (removed). In the second step, for a given  $\tau$ , we consider the process of increasing the asymptotic potential energy difference between channels,  $\nu$ . Every time a bound state of the shallower channel crosses the asymptotic energy of the open channel, we observe an upper channel dominated FR. With increasing  $\nu$ , the coupling becomes less significant and the depths of the channels gradually return to the case of  $\tau = 0$ . During this process, bound states of the deeper channel disappear. Every time a bound state crosses the asymptotic potential energy of the open channel, we observe a lower channel dominated resonance of the scattering length. Hence, the overall number of FRs,  $n_{\text{FR}}$ , for different  $\nu$ , is given by a simple formula,

$$n_{\text{FR}} = n_+ + (n_- - n_o), \quad (29)$$

where  $n_+$  is the number of the bound states in the upper adiabatic potential for  $\nu = 0$ ,  $n_-$  is the number of the bound states in the lower adiabatic potential for  $\nu = 0$ , and  $n_o$  is the number of the bound states in the open channel potential.

## VII. STRONG-COUPLING REGIME

The standard interpretation of FR phenomena applies for weak inter-channel coupling strength  $\tau$ . In this regime, a FR occurs when the closed channel bound state energy approaches the incident energy of the open channel. But at sufficiently high values of the coupling strength, there is a threshold above which yet another kind of FR can appear. This kind of FR occurs for strong coupling strength even when the potential in the closed channel is *repulsive* (or attractive but with no bound state present in the closed channel, as this is possible in 3D). We refer to this as the strong coupling regime.

It was already shown that the tight-binding model reported in Ref. [14] possess the strong coupling regime. Here we demonstrate using the adiabatic representation that the mechanism for creation of this type of FR is similar to the original one, but this time it is a state in a dressed potential that is approaching the threshold rather than the initial bound state in the closed channel potential. We explain this mechanism in detail below.

There are significant differences in how the resonances behave, depending on whether the closed channel potential is attractive, but with no bound states in the closed channel, or repulsive. Therefore, we analyze the two cases separately, starting with the repulsive closed channel potential case.

The expression for the scattering length in Eq. (24) is rather complicated, but the simple formula in Eq. (28) predicts the threshold of the coupling  $\tau$ , above which the

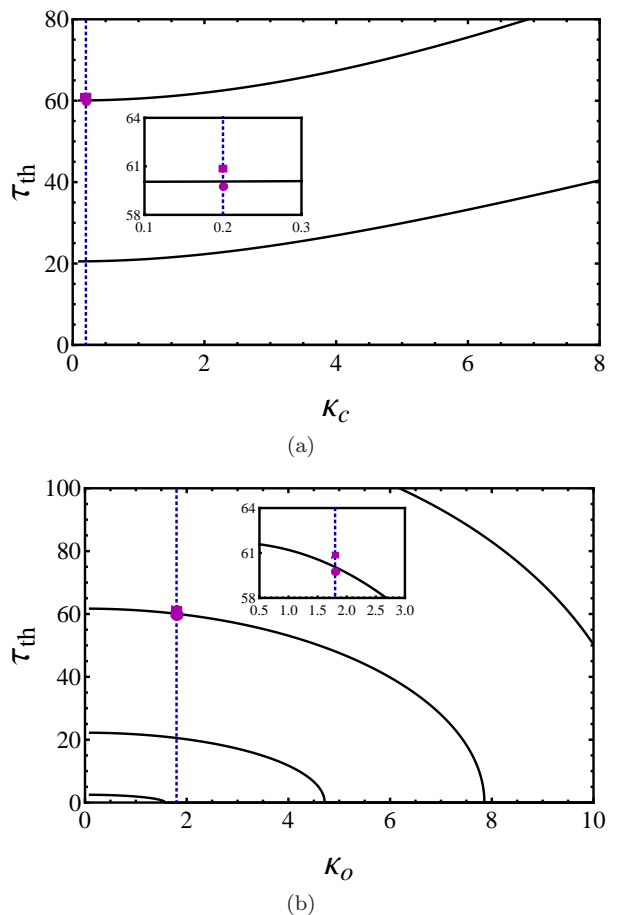


FIG. 3: (Color online) Feshbach resonance for a repulsive potential in the closed channel. (a) Threshold curves (same as in Fig. 6) plotted versus the depth of the closed channel (with  $\kappa_o = 1.8$ ). (b) Threshold curves plotted versus the depth of the open channel (for  $\kappa_c^2 = -0.04$ ). The dashed blue vertical line refers to the numerical calculations where we keep the depth of the potential fixed ( $\kappa_o = 1.8$  and  $\kappa_c^2 = -0.04$ ) and increase the value of  $\tau$  in the analysis illustrated in Figs. 4-5. The purple circle (square) on this line marks the value of  $\tau = 59.75$  ( $\tau = 60.86$ ) which is used in red line in Fig. 4 (black lines in Figs. 4 and 5). Because the circle and square are almost coincide on the scale of the figure, we added an appropriate inset.

new FR appears.

The following formula

$$\tau_{\text{th}}(n^*) = \sqrt{\left(\frac{\pi}{2}\right)^2 (2n^* - 1)^2 + |\kappa_c^2|} \sqrt{\left(\frac{\pi}{2}\right)^2 (2n^* - 1)^2 - \kappa_o^2}, \quad (30)$$

for the threshold value of the coupling strength  $\tau$  for a repulsive closed channel potential can be obtained from Eq. (28) simply by changing  $\kappa_c$  to  $i\kappa_c$ , which corresponds to the change from attractive ( $V_c \geq 0$ ) to repulsive ( $V_c < 0$ ) closed channel potential.

Our results for the case of a repulsive closed channel potential are shown in Figs. 3 through 5. Figure 3 plots a set of solid curves marking the threshold for subsequent

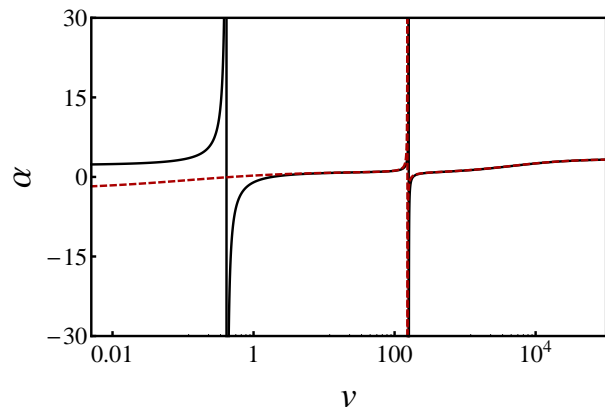


FIG. 4: Scattering length in units of  $r_0$  for a repulsive potential in the closed channel as a function of  $\nu$  (for  $\kappa_c^2 = -0.04$ ). Open channel supports one bound state ( $\kappa_o = 1.8$ ). The dashed red curve shows the scattering length for a coupling strength of  $\tau = 59.75$  (purple circle in Fig. 3) which is below the second threshold at  $\tau_{th} = 60.06$ . The solid black curve is for  $\tau = 60.86$  (purple square in Fig. 3) which is just above the threshold. See also Figs. 5(a) and (b).

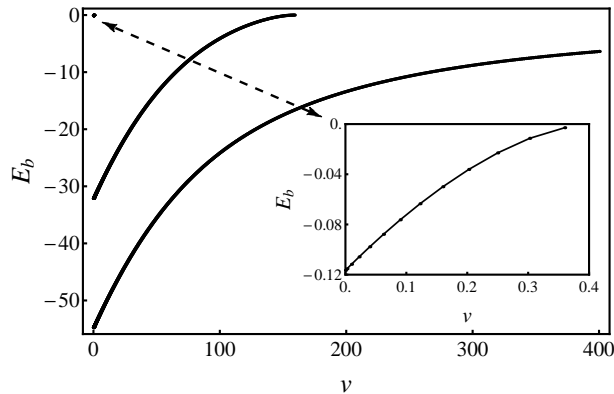


FIG. 5: Energy of the bound states of the coupled system in units of  $\hbar^2/2mr_0^2$  for a repulsive potential in the closed channel ( $\kappa_c^2 = -0.04$ ) as a function of the energy shift  $\nu$  (in the same units as  $E_b$ ). The coupling strength  $\tau = 60.86$ , is just above threshold (purple square in Fig. 3). The inset shows the small  $\nu$  and  $E_b$  region and the dashed two-sided arrow depicts its position.

resonances [see Eq. (30)] versus the depth of the closed [Fig. 3(a),  $\kappa_o = 1.8$ ] and the open channel [Fig. 3(b),  $\kappa_c^2 = -0.04$ ]. First we observe that, due to the coupling, dressed potential picture emerges, and in particular  $V_-$  originates from open channel potential. This potential gets deeper when the interaction strength increases. The exact depth of the dressed potentials depends on both  $\tau$  and  $\nu$ , but when we set  $\nu = 0$  and increase  $\tau$ , a new bound state can appear in  $V_-$ . For each fixed value of  $\tau$  we study what happens to our system with increasing value of the detuning  $\nu$ . In the limit  $\nu \rightarrow \infty$ , the depth of  $V_-$  tends again to  $V_o$  and consequently a new bound state will move towards threshold, eventually crossing it,

thereby creating a FR.

In order to visualize this phenomenon we have drawn a dashed blue vertical line in Figs. 3(a) and (b), referring to the numerical studies summarized in Figs. 4 and 5. Moving vertically up along this line means keeping the depths of the potentials ( $\kappa_o = 1.8$ ,  $\kappa_c^2 = -0.04$ ) fixed and increasing the value of  $\tau$ . Each time a solid curve is crossed, a new FR emerges, due to the mechanism described in the previous paragraph. In Figs. 4 and 5 we included two purple markers, the circle and the square, for the values of  $\tau = 59.75$  and  $\tau = 60.86$ . These values were used in Fig. 4, where we showed the scattering length as a function of  $\nu$ . Notice that there is only one FR for  $\tau = 59.75$ , and two resonances for  $\tau = 60.86$ , in between these two values we crossed one threshold line.

We can gain further insight regarding the mechanism described above from Fig. 5, where we plot energy of the bound states of the coupled system as a function of the detuning  $\nu$ . This figure should be analyzed in parallel with Fig. 4. We notice that FRs appear exactly when bound states of the coupled system disappear. This is also the case when bound states of the potential  $V_-$ , induced by coupling between channels, are pushed through threshold into the continuum.

The situation is slightly more complicated when there is an attractive potential that supports a bound state in the closed channel, although, in general, a similar mechanism applies. The major difference between this and the previous case is the existence of bound states in the closed channel. The detailed analysis is illustrated in Figs. 6 to 8. Figure 6 displays the threshold coupling  $\tau$  at which resonances appear or vanish. In Fig. 6 the closed channel wavevector  $\kappa_c$  is equal 7.5. When we fix both  $\kappa_o = 1.8$ , and  $\kappa_c = 7.5$  and increase the coupling strength, we move along the vertical (blue) dashed line. Taking this path we obtain the results shown in Figs. 7 and 8. These figures show the scattering length versus detuning at two particular values of coupling,  $\tau = 6.3$  and  $\tau = 87.5$ , which are marked with a circle and a square symbol in Fig. 6. We observe that each time a solid curve is crossed in the direction of increasing  $\tau$ , a new FR emerges, and when a black dashed curve is crossed, one of the resonances disappears. Notice that two resonances are present for  $\tau = 6.3$  in Fig. 7(a) and the three resonances for  $\tau = 87.5$  in Fig. 7(b). As shown in Fig. 6, between these values of  $\tau$ , the blue line crosses three threshold curves, i.e., two solid curves and one black dashed curve.

In analogy with the repulsive case, let us now consider the bound states of the coupled system and their dependence on  $\nu$  and  $\tau$ . Again we argue that FRs are associated with the position of the coupled channel bound states. Figure 8(a) shows the energy of the bound states versus the coupling strength  $\tau$  for  $\nu = 0$ . Here we use the same values of  $\kappa_o = 1.8$  and  $\kappa_c = 7.5$  as in Figure 7. We focus our attention on the threshold ( $E_b = 0$ ) and observe that as we increase the coupling strength  $\tau$ , the highest bound state first disappears through the threshold at  $\tau = 6.45$  and then comes back at  $\tau = 17.82$ . One

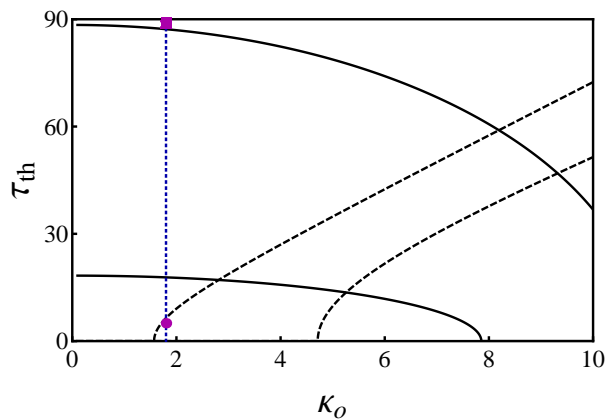


FIG. 6: (Color online) Feshbach resonances in the case of an attractive closed channel potential. The threshold values of the coupling  $\tau$  at which successive resonances appear are plotted as a function of  $\kappa_o$ . Each solid curve plotted versus the depth of the closed channel potential (for fixed value of  $\kappa_c = 7.5$ ) represents one such threshold. When a solid curve is crossed, a new Feshbach resonance emerges and when a black dashed curve is crossed, one resonance disappears. The dashed blue vertical line refers to our numerical studies, as discussed in the text, where the depth of the potentials is held fixed ( $\kappa_o = 1.8$ ,  $\kappa_c = 7.5$ ) and the value of  $\tau$  is increased. The purple circle [square] on this line marks the value of  $\tau = 6.3$  ( $\tau = 87.5$ ) which is used in Figs. 7(a) and 8(a) [Figs. 7(b) and 8(b)].

can check that the former event coincides with one bound state being pushed out of the  $V_+$  well and the former with a new bound state appearing in  $V_-$ . At the right corner of Fig. 8(a) we note the occurrence of one more bound state of the coupled system, again associated with one more bound state pushed into  $V_-$ .

When  $\tau \neq 0$ , it is advantageous to think of Feshbach processes in terms of the adiabatic potentials  $V_+$  and  $V_-$ . Since in this case the closed channel potential well is deeper than the open one,  $V_-$  tends to  $V_c$  as the coupling  $\tau$  approaches zero. For  $\tau = 0$  (no coupling) the open channel dressed potential ( $V_+$ ) supports one bound state and the closed channel dressed potential ( $V_-$ ) supports two bound states. For very small  $\tau$  we expect two FRs as predicted by Eq. 29; they are shown in Fig. 7. But upon increasing  $\tau$  further we cross the first threshold value  $\tau_{\text{th}}$  shown in Fig. 6, and one of the resonances disappear. It happens when the bound state of the coupled system reaches threshold (see inset of Fig. 8), or equivalently, when a bound state in the dressed potential  $V_+$  is pushed into the continuum (remember that with increasing  $\tau$ ,  $V_-$  gets deeper and  $V_+$  gets shallower). As we increase the coupling further, the next threshold is crossed and one additional bound state appears in the  $V_-$  potential and at the same time an additional bound state appears in the coupled channel system (see inset of Fig. 8). If we increase  $\tau$  even further, this pattern repeats; a new bound state is formed (e.g., this occurs at  $\tau = 87.5$ ) in the  $V_-$  potential and in the coupled channel system. In

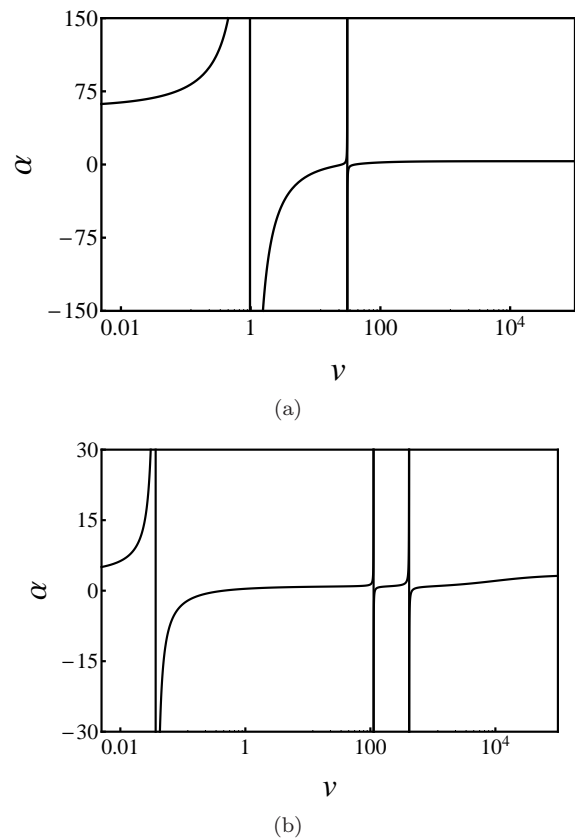


FIG. 7: Scattering length in the units of  $r_0$  as a function of energy shift  $\nu$  in units of  $\hbar^2/(2mr_0^2)$  for an attractive closed channel potential with  $\kappa_c = 7.5$ . Fixed value of  $\kappa_o = 1.8$  corresponds to the case when open channel supports one bound state. Coupling strength is equal to (a)  $\tau = 6.3$  (purple circle in Fig. 6), and (b)  $\tau = 87.5$  (purple square in Fig. 6). Upon increasing the values of coupling strength from (a) to (b) following blue line (see Fig. 6) one passes through three threshold curves. Two new resonances are created upon crossing the two solid lines and one resonance disappears upon crossing the dashed line.

Fig. 7, there are three FRs and three bound states of the coupled system will approach zero when we increase the detuning as can be seen from Fig. 8(b).

## VIII. SUMMARY AND CONCLUSION

The possibility of achieving Feshbach resonance without having a bound-state in the closed channel was suggested in our earlier work, based on a tight-binding model with very simple potentials [14]. In the present work we expand upon that result and show that the concept is robust. Specifically, we studied a piecewise constant potential model and demonstrated that, for strong enough coupling strength, Feshbach resonance occurs even when the closed channel does not have a bound state or even when the closed channel potential is repulsive. Our findings complement and substantially expand upon the analysis of the tight-binding model and the formal scattering theory results reported in Ref. [14]. We introduced a

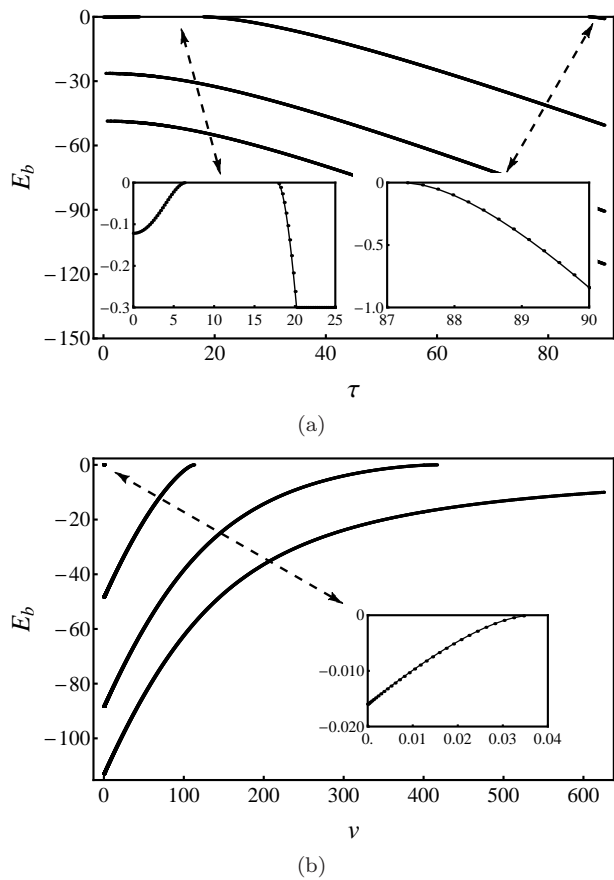


FIG. 8: (a) Energy of the bound states of the coupled system for an attractive potential in the closed channel as a function of the coupling strength  $\tau$  for  $\nu = 0$ . The values of  $\kappa_o$  and  $\kappa_c$  are as in Fig. 7. The inset shows the magnification of the top curve near the origin and reveals that the bound state disappears through the threshold and returns. (b) Energy of the bound states for coupling strength  $\tau = 87.5$  (just above the threshold value; corresponding to purple square in Fig. 6) as a function of the energy shift  $\nu$ . The inset shows the bound state energy for small values of  $\nu$ . All energies are given in units of  $\hbar^2/(2mr_0^2)$ .

dressed potential picture (an adiabatic representation) and elucidated the physical mechanism behind this phenomenon. We derived analytical formulae for the number of Feshbach resonances as a function of the depth of the potentials.

## Acknowledgments

We would like to acknowledge the Foundation for Polish Science International Ph.D. Projects Programme cofinanced by the EU European Regional Development Fund. This research was supported by grants from the the National Science Center (DEC-2011/03/D/ST2/00200, DEC-2011/01/B/ST2/02030 and DEC-2012/07/N/ST2/02879) and the Israel Science Foundation (Nos. 295/2011 and 400/2012).

- 
- [1] J. Faist, *et al.*, *Nature* **390**, 589 (1997); H. Schmidt, K. L. Campman, A. C. Gossard, and A. Imamoglu, *Appl. Phys. Lett.* **70**, 3455 (1997).
  - [2] S. Bar-Ad, P. Kner, M.V. Marquezini, S. Mukamel, D.S. Chemla, *Phys. Rev. Lett.* **78**, 1363 (1997); J. Wagner and M. Cardona, *Phys. Rev. B* **32**, 8071 (1985).
  - [3] M. Kroner, *et al.*, *Nature* **451**, 311 (2008).
  - [4] Ch. Chin, R. Grimm, P. Julienne, and E. Tiesinga, *Rev. Mod. Phys.* **82**, 1225, (2010).
  - [5] T. Köhler, K. Góral and P.S. Julienne, *Rev. Mod. Phys.* **78**, 1311 (2006).
  - [6] H. Feshbach, *Ann. Phys. (N.Y.)* **5**, 357 (1958); *Ann. Phys. (N.Y.)* **19**, 287 (1962); H. Feshbach, *Theoretical Nuclear Physics*, (Wiley, NY, 1992).
  - [7] U. Fano, *Nuovo Cimento* **12**, 154 (1935); *Phys. Rev.* **124**, 1866 (1961).
  - [8] A.J. Moerdijk, B.J. Verhaar, and A. Axelsson, *Phys. Rev. A* **51**, 4852 (1995).
  - [9] E. Timmermans, P. Tommasini, M. Hussein, A. Kerman, *Phys. Rep.* **315**, 199 (1999).
  - [10] D. M. Bauer, M. Lettner, C. Vo, G. Rempe, and S. Durr, *Nat. Phys.* **5**, 339-342 (2009).
  - [11] S. Blatt, *et al.*, *Phys. Rev. Lett.* **107**, 073202 (2011).
  - [12] Z. Li, and R.V. Krems, *Phys. Rev. A*, **75**, 032709, (2007).
  - [13] K. M. Jones, E. Tiesinga, P. D. Lett, and P. S. Julienne, *Rev. Mod. Phys.* **78**, 483-535 (2006).
  - [14] Y. Avishai, Y. B. Band and M. Trippenbach, *Phys. Rev. Lett.* **111**, 155301 (2013).
  - [15] N. W. Ashcroft and N. D. Mermin, *Solid State Physics*, (Holt, Rinehart and Winston, 1976).
  - [16] Y. B. Band and Y. Avishai, *Quantum Mechanics with Applications to Nanotechnology and Information Science*,

- (Elsevier – Academic Press, 2013).
- [17] M. L. Goldberger and K. M. Watson, *Collision Theory*, (Dover, 204), p. 286, Eq. (286).
- [18] R. G. Thomas, Phys. Rev. **88**, 1109 (1952); J. B. Ehrman, Phys. Rev. **81**, 412 (1951).
- [19] M. Krych, W. Skomorowski, F. Pawłowski, R. Moszyński and Z. Idziaszek, Phys. Rev. A **83**, 032723 (2011).
- [20] C. Chin, arXiv:cond-mat/0506313.
- [21] A. D. Lange, K. Pilch, A. Prantner, F. Ferlaino, B. Engeser, H.-C. Nägerl, R. Grimm, C. Chin, Phys. Rev. A **79**, 013622 (2009).
- [22] S. Saeidian, V.S. Melezhik, P. Schmelcher, Phys. Rev. A **86**, 062713 (2012).
- [23] In our case a repulsive potential is a square well potential with a positive short range part.
- [24] Note that the scattering length can be calculated for both  $V > V_{\text{th}}$  and for  $V < V_{\text{th}}$  in terms of the  $s$ -wave scattering phase shift  $\delta(k)$ , where  $k = \sqrt{E}$ . The desired relation for the scattering length is  $a = -\lim_{k \rightarrow 0} \tan \delta(k)/k$ . For  $V > V_{\text{th}}$ ,  $\delta(0) = n\pi$  and  $a = -[d\delta/dk]_{k \rightarrow 0}$ , which is approximately equal to  $\hbar/\sqrt{2m|E_b|}$ . On the other hand, for the case of zero energy resonance ( $V \rightarrow V_{\text{th}}$  from below),  $\delta(0) = (n + \frac{1}{2})\pi$  and, strictly speaking,  $a \rightarrow -\infty$ . When the expression  $-\tan \delta(k)/k$  is employed at finite but small  $k$ ,  $a$  is very large and negative.